Equilibrium phase diagram of a randomly pinned glass-former

Misaki Ozawa[a,b], Walter Kob[c,1], Atsushi Ikeda[d], and Kunimasa Miyazaki[b]

[a]Institute of Physics, University of Tsukuba, Tsukuba 305-8571, Japan; [b]Department of Physics, Nagoya University, Nagoya 464-8602, Japan; [c]Laboratoire Charles Coulomb, UMR 5221, University of Montpellier and CNRS, 34095 Montpellier, France; and [d]Fukui Institute for Fundamental Chemistry, Kyoto University, Kyoto 606-8103, Japan

Edited by Pablo G. Debenedetti, Princeton University, Princeton, NJ, and approved April 16, 2015 (received for review January 13, 2015)

We use computer simulations to study the thermodynamic properties of a glass-former in which a fraction c of the particles has been permanently frozen. By thermodynamic integration, we determine the Kauzmann, or ideal glass transition, temperature $T_K(c)$ at which the configurational entropy vanishes. This is done without resorting to any kind of extrapolation, i.e., $T_K(c)$ is indeed an equilibrium property of the system. We also measure the distribution function of the overlap, i.e., the order parameter that signals the glass state. We find that the transition line obtained from the overlap coincides with that obtained from the thermodynamic integration, thus showing that the two approaches give the same transition line. Finally, we determine the geometrical properties of the potential energy landscape, notably the T- and c dependence of the saddle index, and use these properties to obtain the dynamic transition temperature $T_d(c)$. The two temperatures $T_K(c)$ and $T_d(c)$ cross at a finite value of c and indicate the point at which the glass transition line ends. These findings are qualitatively consistent with the scenario proposed by the random first-order transition theory.

ideal glass transition | computer simulations | random first-order transition theory | Kauzmann temperature | configurational entropy

Upon cooling, glass-forming liquids show a dramatic increase of their viscosities and relaxation times before they eventually fall out of equilibrium at low temperatures (1, 2). This laboratory glass transition is a purely kinetic effect because it occurs at the temperature at which the relaxation time of the system crosses the time scale imposed by the experiment, e.g., via the cooling rate. Despite the intensive theoretical, numerical, and experimental studies of the last five decades, the mechanism responsible for the slowing down and thus for the (kinetic) glass transition is still under debate and hence a topic of intense research. From a fundamental point of view the ultimate goal of these studies is to find an answer to the big question in the field: Does a finite temperature exist at which the dynamics truly freezes and, if so, is this ideal glass transition associated with a thermodynamic singularity or is it of kinetic origin (3–6)?

Support for the existence of a kinetic transition comes from certain lattice gas models with a "facilitated dynamics" (6). In these models, the dynamics is due to the presence of "defects" and hence for such systems the freezing is not related to any thermodynamic singularity. However, the first evidence that there does indeed exist a thermodynamic singularity goes back to Kauzmann, who found that the residual entropy (the difference of the entropy of the liquid state from that of the crystalline state) vanishes at a finite temperature T_K if it is extrapolated to temperatures below the laboratory glass transition (7). Subsequently many theoretical scenarios that invoke the presence of a thermodynamic transition have been proposed (8–10). One of these is the so-called "random first-order transition" (RFOT) theory which, inspired by the exact solution of a mean-field spin glass, predicts that at T_K the glass-former does indeed undergo a thermodynamic transition at which the residual, or configurational entropy S_c (the logarithm of the number of the states which are available to the system) vanishes and concomitantly breaks the replica symmetry (10, 11). A further appealing feature of RFOT is that it seems to reconcile in a natural way the (free) energy-landscape scenario and mode-coupling theory (MCT), a highly successful theory that describes the relaxation dynamics at intermediate temperatures (12).

Despite all these advances, the arguments put forward in the various papers must be considered as phenomenological because compelling and undisputed experimental or numerical evidence to prove or disprove any of these theories and scenarios is still lacking. The only exception is hard spheres in infinite dimensions, for which mean-field theory should become exact (13), but even in this case some unexpected problems are present (see ref. 14). This lack of understanding is mainly due to the steep increase of the relaxation times which hampers the access to the transition point of thermally equilibrated systems, and hence most of the efforts to identifying the transition point, if it exists, resort to unreliable extrapolation.

Randomly Pinned Systems

Recently a novel idea to bypass this difficulty has been proposed (15–18). By freezing, or pinning, a fraction of the degrees of freedom of the system, the ideal glass transition temperature has been predicted to rise to a point at which experiments and simulations in equilibrium are feasible, thus allowing one to probe the nature of this transition. In ref. 15 the authors have studied the effect of pinning for the case of a mean-field spin-glass model which is known to exhibit a dynamical MCT transition at a temperature T_d and a thermodynamic transition at a lower temperature T_K. It was demonstrated that by pinning a fraction c of the degree of freedoms of the spins (selected at random) in the equilibrated system, both $T_K(c)$ and $T_d(c)$ increase with c. Thus, by equilibrating the nonpinned system at an intermediate temperature and subsequently increasing c, one can access and probe the ideal

Significance

Confirming by experiments or simulations whether or not an ideal glass transition really exists is a daunting task, because at this point the equilibration time becomes astronomically large. Recently it has been proposed that this difficulty can be bypassed by pinning a fraction of the particles in the glass-forming system. Here we study numerically a liquid with such random pinned particles and identify the ideal glass transition point T_K at which the configurational entropy vanishes, thus realizing for the first time, to our knowledge, a glass with zero entropy. We find that as the fraction of pinned particles increases, the T_K line crosses the dynamical transition line, implying the existence of an end point at which theory predicts a new type of criticality.

Author contributions: M.O., W.K., A.I., and K.M. designed research, performed research, analyzed data, and wrote the paper.

The authors declare no conflict of interest.

This article is a PNAS Direct Submission.

[1]To whom correspondence should be addressed. Email: walter.kob@univ-montp2.fr.

This article contains supporting information online at www.pnas.org/lookup/suppl/doi:10.1073/pnas.1500730112/-/DCSupplemental.

glass state in thermal equilibrium [Note that changing c does not perturb this equilibrium (19).] It was found that at sufficiently large c the two lines $T_K(c)$ and $T_d(c)$ merge and terminate at a critical point with a universality class of the random-field Ising model (15, 20).

Very recently, it has been tested whether this approach to detect T_K in mean-field models can also be used in realistic glass-formers in finite dimensions (21). It was found that pinned systems do indeed show a behavior that agrees qualitatively with the theoretical predictions, thus giving encouraging evidence that the nature of the ideal glass transition can be studied in equilibrium. In these numerical studies, the overlap q and its distribution $[P(q)]$ have been used to identify the amorphous-fluid phase diagram in the T–c plane for pinned systems (21).

Despite these results, it is not clear if the so-obtained amorphous state is the bona fide ideal glass for which the configurational entropy S_c vanishes and, in view of the conceptual importance of S_c, this is a very disturbing situation. We recall that S_c is related to the number of available states of the system (10, 11) and is also a key quantity that controls the slow dynamics in the activation regime in which the relaxation time τ_α is related to S_c via the Adam–Gibbs relation, $\ln \tau_\alpha \propto 1/TS_c$ (10, 22). Finally, S_c is intimately related to the Landau-like free energy associated with the overlap of two coupled replicas (23).

Although from the simulations reported in ref. 21 the existence of T_K has been inferred from the behavior of the overlap distribution $[P(q)]$ (discussed in more detail below), such an analysis of the overlap q alone may not be conclusive to demonstrate the existence of the arrested phase, because one cannot exclude the possibility that other scenarios, such as the purely kinetic one, can also explain the observed features of $[P(q)]$. Thus, evaluating S_c directly and identifying the temperature at which it vanishes is crucial to disentangle conflicting theoretical scenarios.

In the present work, we use computer simulation to determine the ideal glass transition temperature $T_K(c)$ as a point at which S_c vanishes for a canonical glass-former with pinned particles. For the first time, to our knowledge, this is done without invoking any kind of extrapolation. We also calculate the overlap distribution $[P(q)]$ and find that T_K obtained from $S_c(T_K) = 0$ and from $[P(q)]$ agree very well up to a finite value of c. Furthermore, we analyze the geometrical properties of the potential energy landscape (PEL) and use it to evaluate the dynamic transition temperature $T_d(c)$ as a point at which the saddles of the energy landscape vanish. We find that $T_d(c)$ merges with $T_K(c)$ exactly at the point at which the two mentioned $T_K(c)$ depart from each other, strongly indicating the existence of a critical point which is predicted by the mean-field analysis (15–17).

Results

We study a standard glass-forming model: A 3D binary Lennard-Jones mixture (24). The number of particles is $N = 150$ and 300, but most of the results are for $N = 300$ (see *Materials and Methods* for details). Throughout the present study, the system has been prepared at each temperature by randomly choosing a fraction c of particles from the thermally equilibrated samples and quenching their positions (see *Materials and Methods* for details).

Entropy and Configurational Entropy. To obtain the entropy of the pinned system S, we used thermodynamic integration to determine the entropy of a given configuration of pinned particles and subsequently calculated S by averaging over the realizations of pinned particles (see *Materials and Methods* for details).

Fig. 1*A* shows the entropy per (unpinned) particle $s \equiv S/N(1-c)$. as a function of the fraction of pinned particles at several temperatures T, and we recognize that with increasing c the entropy decreases rapidly. For all temperatures this decrease is linear at small c but then the curves bend at intermediate c and follow a weaker

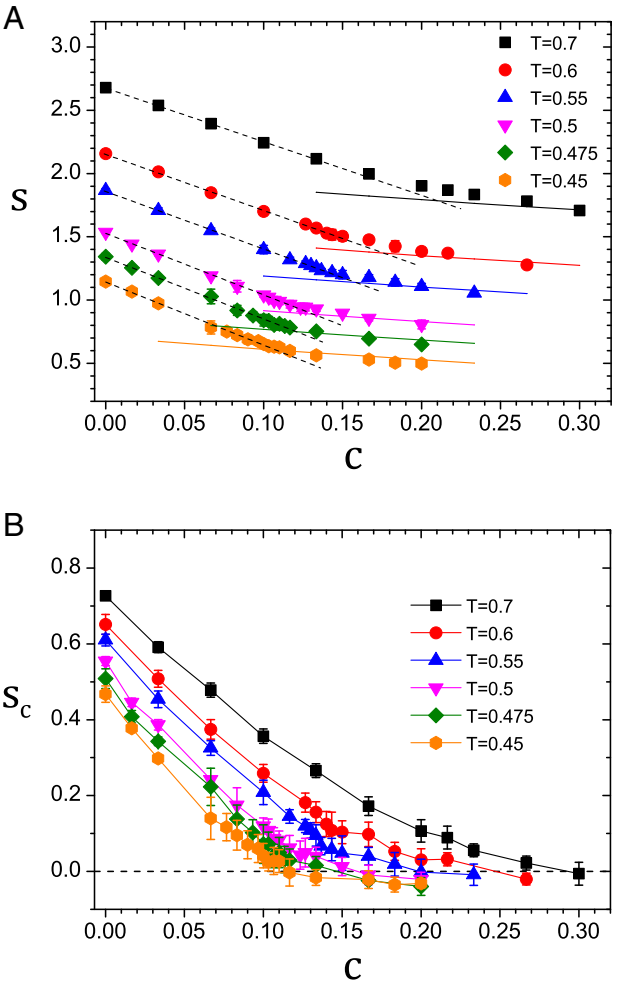

Fig. 1. (*A*) Entropy of the system, s, as evaluated from the thermodynamic integration, as a function of c (symbols). The entropies of the disordered solid states s_{vib}, obtained using the harmonic approximation, are drawn as solid lines. The dashed lines are a linear extrapolation from the low-c sides. (*B*) The configurational entropy $s_c = s - s_{vib}$. The error bars have been estimated from the sample-to-sample fluctuations.

c dependence. For $T \lesssim 0.5$ this bent becomes sharp, strongly indicating that a thermodynamic glass transition takes place.

This becomes more evident by evaluating the configurational entropy obtained by subtracting from S the vibrational entropy S_{vib}. To estimate S_{vib}, we have determined the inherent structures (25) and calculated the eigenfrequencies ω_a. Using the harmonic approximation, one can then approximate $S_{vib} = \sum_a \{1 - \log(\beta\hbar\omega_a)\}$. $s_{vib} \equiv S_{vib}/N(1-c)$ is shown in Fig. 1*A* as well (solid lines) and we see that it shows basically a linear decrease with c, a trend which is due to the suppression of the low-frequency modes in the density of states.

We can now estimate the configurational entropy S_c as the difference $S_c = S - S_{vib}$ (26) and in Fig. 1*B* we show the c dependence of $s_c = S_c/N(1-c)$ for various temperatures. This figure shows that, for $T \lesssim 0.5$, s_c quickly decreases with increasing c and becomes basically zero at a finite value of c, indicating that the system has entered the ideal glass state in which the entropy is basically due to harmonic vibrations. [The fact that the difference $s - s_{vib}$ is slightly negative is related to the harmonic approximation used to estimate s_{vib}. We have estimated the anharmonic correction to s_{vib} by considering the nonlinear contribution of the potential energy at the inherent structures (27) and found that the corrections are very small and negative.

Evaluation of the exact values of this correction is, however, difficult and beyond the scope of the present work. In principle, one can avoid this difficulty by evaluating the configurational entropy directly (28). However, at present such an approach is computationally way too expensive for systems close to the ideal glass transition.] For $T \gtrsim 0.55$, the approach of s_c to zero is milder and the bent is less sharp, indicating that the transition becomes a cross-over.

We define the ideal glass transition point $c_K(T)$, or $T_K(c)$, as the point at which s_c becomes zero. As the temperature is lowered, $c_K(T)$ decreases and we show the resulting phase diagram, the details of which will be discussed below in Fig. 4. Finally, we mention that the presented results are for $N = 300$. However, we have also simulated systems with $N = 150$ and found that the results do not depend significantly on N (see *SI Text* for details).

Overlap Approach. An alternative method to locate and characterize the thermodynamic transition is to study the overlap $q_{\alpha\beta}$ between two configurations α and β: $q_{\alpha\beta} = N^{-1}\sum_{i,j}\theta(a - |\mathbf{r}_i^\alpha - \mathbf{r}_j^\beta|)$, where θ is the Heaviside function, $\mathbf{r}_i^\alpha$ is the position of particle i in configuration α, and the length scale a is 0.3 (21). RFOT predicts that at the glass transition the average value $[\langle q\rangle]$ will increase quickly from a small value in the fluid phase to a large value in the glass phase (16). Here $\langle\cdots\rangle$ and $[\cdots]$ stand for the thermal and disorder averages, respectively. We have computed the overlap distribution $P(q)$ using replica exchange molecular dynamics (21) (*SI Text*) and in Fig. 2 we present $[P(q)]$ for $T = 0.7$ and 0.45. For $T = 0.7$, $[P(q)]$ remains single-peaked for all c, and the peak position shifts continuously toward larger q as c increases (Fig. 2*A*). A qualitatively different behavior is observed at $T = 0.45$ (Fig. 2*B*): $[P(q)]$ is single-peaked at low and high c, but has a double-peak structure at intermediate c, thus signaling the coexistence of the fluid and glass phase, which indicates that the transition from the fluid phase to the glass phase is first-order–like (21).

The c dependence of the average overlap $[\langle q\rangle]$ is shown in Fig. 2*C*. For high temperatures, $T \gtrsim 0.6$, $[\langle q\rangle]$ smoothly increases with c, reflecting the continuous shift of the single peak of $[P(q)]$ as shown in Fig. 2*A*. For $T \lesssim 0.5$, $[\langle q\rangle]$ shows a quick increase at intermediate values of c, in agreement with the presence of the double-peak structure seen in $[P(q)]$ at these T. It suggests that a first-order–like transition, rounded by finite size effect, takes place, in qualitative agreement with the result for a system of harmonic spheres (21). Note that, within the accuracy of our data, we see that the amplitude of the (smeared out) jump in $[\langle q\rangle]$ seems to vanish around $0.55 \lesssim T \lesssim 0.6$, thus indicating that at around that temperature the line of first-order transition ends in a critical point that is second-order–like.

From this approach with the overlap, we can define the ideal glass transition temperature $T_K^{(q)}(c)$ as the temperature at which the skewness of $[P(q)]$ vanishes (*SI Text*), and in Fig. 4 we have included the resulting $T_K^{(q)}(c)$ as well. For small and intermediate c, we find a very good agreement between $T_K(c)$ and $T_K^{(q)}$, thus showing that the two very different approaches do give the same ideal glass transition temperature. This is thus very strong evidence that at this temperature the system does indeed undergo a thermodynamic phase transition from the fluid to an ideal glass state. For temperatures above the second-order–like critical point the curves $T_K(c)$ and $T_K^{(q)}(c)$ differ. We will rationalize this in *Discussion* below. Finally, we mention that the curves $T_K(c)$ and $T_K^{(q)}(c)$ seem to extrapolate in a smooth manner to the Kauzmann temperature of the bulk which has been estimated from extrapolation (26). This shows that the present measurement of the bulk T_K is compatible with the one from previous estimates.

PEL and MCT. In the past, it has been found that the slow dynamics of glass-forming systems is closely related to the features of the PEL (27) and in the following we will use these relations to characterize the relaxation dynamics of the pinned system.

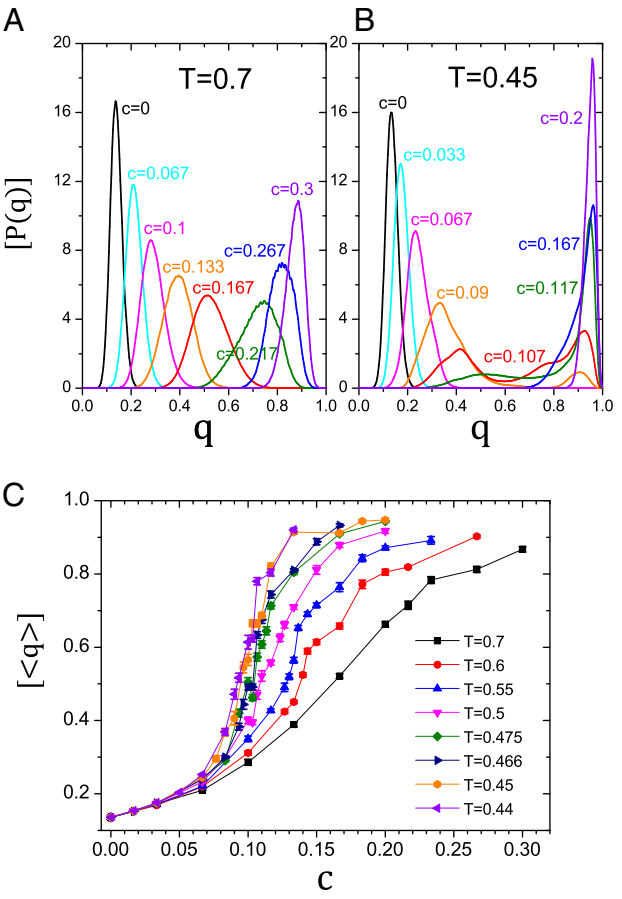

Fig. 2. Distribution of the overlap $[P(q)]$ for $T = 0.7$ (*A*) and $T = 0.45$ (*B*). (*C*) The average overlap $[\langle q\rangle]$ obtained from $[P(q)]$ as a function of c for several temperatures. The error bars have been calculated using the jackknife method.

Fig. 3*A* shows the T dependence of the average inherent structure energy $[\langle e_{IS}\rangle]$. For the bulk system, $c = 0$, $[\langle e_{IS}\rangle]$ is basically constant at high temperatures but then steeply decreases below a cross-over temperature $T \approx 1$, a temperature which signals that the relaxation dynamics becomes strongly influenced by the PEL (29, 30). As c increases, the value of $[\langle e_{IS}\rangle]$ at high T moves steadily upward, which is reasonable because the energy of the system is literally pinned at the higher energy levels due to the presence of the pinned particles. Concomitantly the cross-over temperature increases with c and the cross-over becomes smeared out, completely disappearing at the highest c. The vanishing of this cross-over with growing c indicates thus that the pinning qualitatively affects the nature of the PEL and of the relaxation dynamics. For instance, it is found that with increasing c the fragility of the system decreases and shows at high c an Arrhenius dependence (21, 31).

In Fig. 3*A*, *Inset*, the low-temperature behavior of $[\langle e_{IS}\rangle]$ is shown. It clearly demonstrates that $[\langle e_{IS}\rangle]$ is inversely proportional to T for all c. According to the energy landscape scenario, this is an indicator that the distribution of e_{IS} is Gaussian (32).

Another important quantity that connects the glassy dynamics of a system with its PEL is the saddle index K, i.e., the number of negative eigenvalues of the Hessian matrix at a stationary point of the PEL. For bulk systems it has been found that K shows a linear dependence on e_{SP}, the bare energy of a saddle point (33, 34). Because the value of e_{SP} at which K goes to zero (this value is often denoted as "threshold energy" e_{th}) corresponds to the average energy of the inherent structures $\langle e_{IS}\rangle$ at the critical temperature of MCT, one can extract from the geometrical properties of

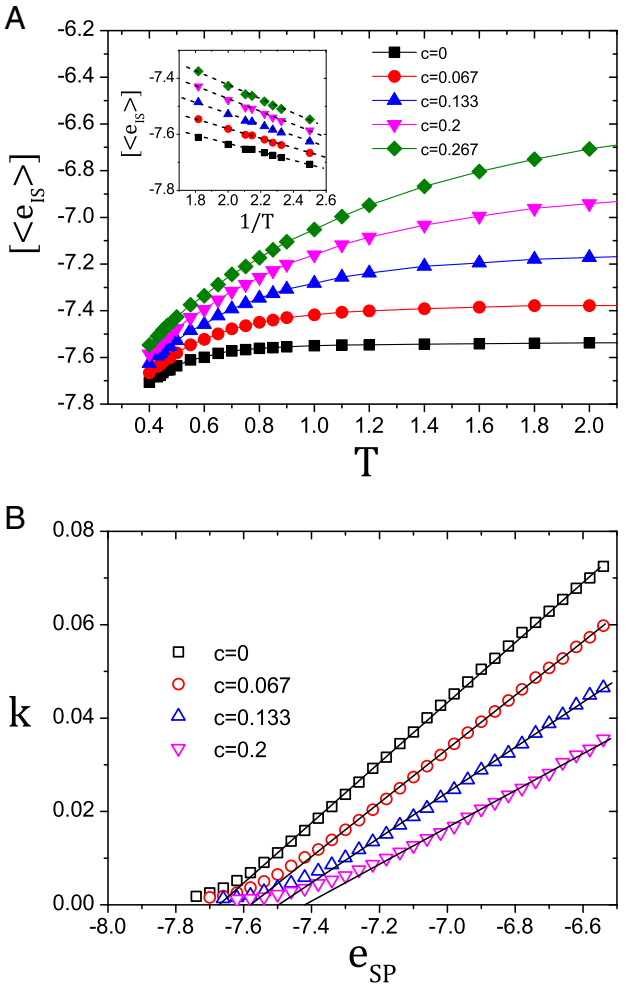

Fig. 3. (*A*) T dependence of the averaged inherent structure $[\langle e_{IS}\rangle]$ for several values of c. (*Inset*) Same quantity as a function of $1/T$. (*B*) The average normalized saddle index k as a function of its energy e_{SP} for several values of c. The threshold energy e_{th} is defined by a linear extrapolation from the high-energy side.

the PEL the value of T_d without having to do any fit to dynamical data (33, 34).

We use a standard method to determine numerically the energy and index of saddles for the pinned system (see *SI Text* for details), and in Fig. 3*B* we plot the average normalized saddle index $k = K/3N(1-c)$ as a function of its corresponding e_{SP}. In agreement with previous studies of the PEL, we find that k decreases linearly as a function of e_{SP} and hence we can obtain $e_{th}(c)$ from a linear fit (included in the figure as well). We see immediately that e_{th} increases with c and, together with the data of Fig. 3*A* and $e_{th}(c) = [\langle e_{IS}\rangle](T_d(c))$, we can conclude that $T_d(c)$ increases with c. The resulting c dependence of T_d is included in Fig. 4 as well and will be discussed in the next section.

We have also evaluated T_d by calculating the relaxation time τ_α from the time-dependent density correlation function (*Material and Methods*) and by fitting τ_α with the MCT power law $\tau_\alpha \propto \left|T - T_d^{(\mathrm{fit})}\right|^{-\gamma}$. We find that the so-obtained values of $T_d^{(\mathrm{fit})}$ agree well with those obtained from the PEL (see *SI Text* for details). Note that one needs several fit parameters to obtain $T_d^{(\mathrm{fit})}$ from the dynamic data, whereas basically no fit parameters are required for T_d from the PEL. In Fig. 4, the iso-τ_α lines are also plotted. The graph shows that τ_α quickly increases with c and that the lines asymptotically approach the T_K line from the high-T side.

Discussion

In Fig. 4 we summarize the results of the previous sections in the form of a phase diagram in the c–T plane. The ideal glass transition lines $T_K(c)$ determined from $S_c = 0$ and $T_K^{(q)}(c)$ obtained from $[P(q)]$ are plotted as filled circles and diamonds, respectively. At low T and c the two temperatures basically coincide but around $(T_c, c_c) \approx (0.55, 0.16)$ they start to depart from each other in that $T_K^{(q)}(c)$ increases continuously, whereas $T_K(c)$ bends and its c dependence becomes weaker. Note that this separation occurs at the same point at which $[P(q)]$ changes from the bimodal to the single-peaked shape (Fig. 2), thus indicating that in this region of parameter space the system has a second-order–like critical point.

The theoretical calculations for a mean-field spin-glass model show that $T_K(c)$ should terminate at a finite c and that this end point is a critical point of the universality class of the random field Ising model (15–17, 20). Furthermore, the theory predicts that at this end point the coexistence line $T_K(c)$ and the dynamical line $T_d(c)$ merge. Fig. 4 shows that this prediction is indeed compatible with our data in that the two lines do cross near (T_c, c_c).

From the figure we also recognize that, beyond the end point, $T_K(c)$ obtained from $S_c = 0$ almost matches with $T_d(c)$. This result is reasonable because in this range of T and c the particles are strongly confined by the labyrinthine structure imposed by the pinned particles, i.e., the system resides mainly at the bottom of a free-energy minimum where both the configurational entropy and the number of the saddles vanish simultaneously. In contrast with $T_K(c)$, $T_K^{(q)}(c)$ raises continuously even beyond the end point. This can be understood by recalling that this line is defined by the points at which the skewness becomes zero, i.e., the point at which $[P(q)]$ changes from being left-skewed to right-skewed. Because this change of sign in the skewness occurs also in the region of the phase diagram beyond the critical point, the line $T_K^{(q)}$ will extend into that region, similar to the Widom line present in a standard liquid–gas transition (35, 36).

As it is evident from Fig. 1*A*, T_K, defined as the point at which $S_c = S - S_{vib} = 0$, becomes somewhat ill-defined beyond the end point ($T \gtrsim 0.55$ in Fig. 1*A*), because the cross-over from the fluid to the glass phase becomes broad. To estimate the effect of this

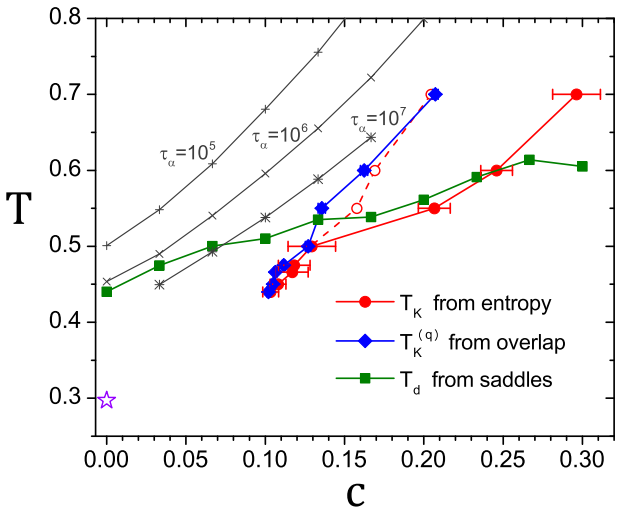

Fig. 4. Phase diagram of the randomly pinned system. The filled circles show the ideal glass line T_K at which the configurational entropy vanishes. The diamonds show $T_K^{(q)}(c)$ determined from the skewness of $[P(q)]$. The squares are dynamic transition points $T_d(c)$. The open circles show the ideal glass line T_K' determined by the linear extrapolation of $S_c(c)$ to vanish from Fig. 1*B*. The iso-relaxation times are drawn by +, ×, and *. The star denoted at $c = 0$ is a putative ideal glass transition point $T_K \approx 0.3$ for the bulk reported in ref. 26.

ambiguity, we have also included in Fig. 4 T_K' defined by the linear extrapolation S_c of Fig. 1*B* from the low-c side (open circles). We see that below the end point $T \lesssim 0.5$, T_K' is indistinguishable from T_K, whereas beyond the end point, $T \gtrsim 0.6$, they bifurcate and T_K' becomes comparable with $T_K^{(d)}$.

To the best of our knowledge, the present study is the first report of a system in finite dimensions that shows the existence of an ideal glass state in equilibrium, i.e., a state in which the configurational entropy is zero at a finite T. The Kauzmann temperatures reported in the past have all relied on somewhat questionable extrapolation procedures, leaving thus room for debate over the very existence of a thermodynamic transition (6, 8, 37).

Our findings are inconsistent with recent simulation studies in which the T- and c dependence of the relaxation dynamics has been studied (38). In ref. 38, the structural relaxation time τ_α was fitted with the Vogel–Fulcher relation $\tau_\alpha \sim \exp[A/(T-T_0)]$, with T_0 as fit parameter. This relation can be directly derived from the Adam–Gibbs as well as the RFOT theory, both of which assert that $\ln \tau_\alpha \propto 1/TS_c$, and thus the Vogel–Fulcher temperature T_0 is predicted to be identical to T_K. Furthermore, the authors of ref. 38 fitted their data also with the MCT power law $\tau_\alpha \propto |T-T_d|^{-\gamma}$ to determine the c dependence of T_d. It was found that whereas T_d increases moderately with c, T_0 remains constant. We have plotted the relaxation time τ_α as a function of S_c for finite c and found that the Adam–Gibbs relation is violated (see *SI Text* for details). Thus, we conclude that in the case of pinned systems one cannot deduce the Vogel–Fulcher law from the Adam–Gibbs relation.

Because the results presented here are all obtained in thermodynamic equilibrium without referring to any kind of extrapolation, we are confident that the phase diagram presented in Fig. 4 does indeed reflect the properties of the system and is not an artifact of the analysis. Further evidence that the simulated system is really in equilibrium is the observation that the entropy obtained by thermodynamic integration from the high-temperature limit matches with that obtained from the low-temperature side (via harmonic approximation) in the glass phase. It is also reassuring that all three methods, the thermodynamic integration (vanishing entropy), the overlap distribution (the discontinuous jump of q), and the geometric change of the PEL, consistently point to the same end point, thus giving strong evidence that this point really exists. Also suggestive is that each combination of pairs among the three methods is compatible beyond the end point, which is reminiscent of the Widom line in the standard gas–liquid phase transition.

At this stage we can conclude that the phase diagram as predicted by the RFOT theory is confirmed at least qualitatively. What remains to be done is to probe the relaxation dynamics in the vicinity of the critical end point because one can expect that this dynamics is rather unusual (39) and to establish its universality class (20, 40). Furthermore, it will also be important to see whether the predicted phase diagram can also be observed in real experiments. Although this will be not easy, for certain systems such as colloids or granular media it should be possible.

Materials and Methods

Model. The system we use is a binary mixture of Lennard-Jones particles (24). Both species A and B have the same mass and the composition ratio is $N_A:N_B = 80:20$. The interaction potential between two particles is given by $v_{\alpha\beta}(r) = 4\epsilon_{\alpha\beta}\{(r/\sigma_{\alpha\beta})^{12} - (r/\sigma_{\alpha\beta})^{6}\}$, where $\alpha, \beta \in \{A, B\}$. We set $\epsilon_{AA} = 1.0$, $\epsilon_{AB} = 1.5$, $\epsilon_{BB} = 0.5$, $\sigma_{AA} = 1.0$, $\sigma_{AB} = 0.8$, and $\sigma_{BB} = 0.88$. $v_{\alpha\beta}(r)$ is truncated and shifted at $r = 2.5\sigma_{\alpha\beta}$. We show energy in units of ϵ_{AA}, with the Boltzmann constant $k_B = 1$, and length in units of σ_{AA}. Time units are defined by Monte Carlo sweeps (see below). Simulations are performed at constant density $\rho \approx 1.2$. The number of particles is $N = 150$ and 300, and most of the results in the present study are for $N = 300$.

Making Pinned Configurations. The configuration of the pinned particles is generated by making first a replica exchange run for the bulk system, i.e., $c = 0$, using eight replicas (41). This allows us to generate relatively quickly many equilibrium configurations that are completely independent, i.e., between consecutive configurations the mean-squared displacement of a tagged particle is more than 100. Next we use a "template" to identify the cN particles that will be permanently pinned. Details on how to create the template can be found in ref. 21. This approach has the advantage that the pinned particles cover the space in a relatively uniform manner, thus avoiding the creation of dense regions or large empty regions and hence suppressing strong sample-to-sample fluctuations of the thermodynamic properties of the system.

Simulation Methods.

Thermodynamics. To sample thermodynamic properties efficiently at low-T and large-c region, we use the replica exchange method (41). The maximum number of replicas is 24. More detail is presented in *SI Text* and in ref. 21. The total CPU time to obtain the presented results is about 580 y of single core time.

Dynamics. We use the Monte Carlo (MC) dynamics simulation to calculate dynamical observables (42). The rule of the MC dynamics is the following: In an elementary move, one of the $(1-c)N$ unpinned particles is chosen at random. Then the particle is displaced at random within a cubic box of linear size $\delta = 0.15$ and the standard Metropolis rule is used to decide whether or not the move is accepted. One MC step consists of $(1-c)N$ such attempts and we set this as a unit of time scale. The relaxation time τ_α is determined by $F_s^A(k, \tau_\alpha) = e^{-1}$, where $F_s^A(k, t)$ is the self part of the intermediate scattering function of the free particles of species A for the wave vector k at the peak of the corresponding structure factor. We have averaged over 20–30 different realizations of pinned particles to calculate $F_s^A(k, t)$.

Entropy. To calculate the entropy $S(c, T)$ of the pinned system, we have first determined the entropy of the system for a given configuration of pinned particles, and then taken the average over the realization of the configuration of pinned particles. For this we have calculated the potential energy at temperatures ranging from the target temperature up to the ideal gas limit at $T = \infty$, while keeping the pinning configuration fixed. We have evaluated the entropy of the system with that pinning configuration using thermodynamic integration. For this integration, we have used a grid in the inverse temperature $\beta = 1/T$ of width $\Delta\beta$ that ranged between 0.01 and 0.1, depending on the temperature, and integrated the potential energy as a function of β. Special care was taken in the very high temperature regime, to accurately and rapidly achieve the convergence to high-temperature ideal gas limit. The high-temperature expansion of the potential energy of Lennard-Jones fluid can be written as $U = A\beta^{-1/4} + B\beta^{-2/4} + C\beta^{-3/4}$ (43). We have used simulations at very high temperatures to determine the coefficients A, B, and C, and then carried out the thermodynamic integration analytically.

Analysis of the Saddles. To locate the saddles of the PEL of the system, we have made a minimization of the squared gradient potential $W = 1/2|\nabla U|^2$ (33, 34). Minimization of W is performed by the Broyden–Fletcher–Goldfarb–Shanno algorithm (44). Similar to the minimization of U used to calculate the inherent structures, W includes the position of the pinned as well as unpinned particles, but only the position of the latter is optimized. After having located a saddle with energy e_{SP}, the Hessian matrix was diagonalized and we counted the fraction of negative eigenvalues $k(e_{SP})$. The raw data are shown in *SI Text* and in Fig. 3*B* we present the average index as a function of e_{SP}. The threshold energy e_{th} is defined by $k(e_{th}) = 0$.

ACKNOWLEDGMENTS. We thank G. Biroli, C. Cammarota, D. Coslovich, and K. Kim for helpful discussions. M.O. acknowledges the financial support by Grant-in-Aid for Japan Society for the Promotion of Science Fellows (26.1878). W.K. acknowledges the Institut Universitaire de France. A.I. acknowledges JSPS KAKENHI 26887021. K.M. and M.O. acknowledge KAKENHI 24340098, 25103005, 25000002, and the JSPS Core-to-Core Program. The simulations have been done in Research Center for Computational Science, Okazaki, Japan, at the HPC@LR, and the CINES (Grant c2014097308).

1. Debenedetti PG, Stillinger FH (2001) Supercooled liquids and the glass transition. *Nature* 410(6825):259–267.
2. Binder K, Kob W (2011) *Glassy Materials and Disordered Solids* (World Scientific, Singapore).
3. Cavagna A (2009) Supercooled liquids for pedestrians. *Phys Rep* 476(4):51–124.
4. Berthier L, Biroli G, Bouchaud J-P, Cipelletti L, van Saarloos W (2011) *Dynamical Heterogeneities in Glasses, Colloids, and Granular Media* (Oxford Univ Press, Oxford).

5. Berthier L, Biroli G (2011) Theoretical perspective on the glass transition and amorphous materials. *Rev Mod Phys* 83(2):587–645.
6. Chandler D, Garrahan JP (2010) Dynamics on the way to forming glass: Bubbles in space-time. *Annu Rev Phys Chem* 61:191–217.
7. Kauzmann W (1948) The nature of the glassy state and the behavior of liquids at low temperatures. *Chem Rev* 43(2):219–256.
8. Tarjus G (2011) An overview of the theories of the glass transition. *Dynamical Heterogeneities in Glasses, Colloids, and Granular Media*, eds Berthier L, Biroli G, Bouchaud J-P, Cipelletti L, van Saarloos W (Oxford Univ Press, Oxford).
9. Tanaka H (2011) Roles of bond orientational ordering in glass transition and crystallization. *J Phys Condens Matter* 23(28):284115.
10. Biroli G, Bouchaud J-P (2012) The random first-order transition theory of glasses: A critical assessment. *Structural Glasses and Supercooled Liquids: Theory, Experiment, and Applications*, eds Wolynes PG, Lubchenko V (Wiley, New York).
11. Kirkpatrick TR, Thirumalai D, Wolynes PG (1989) Scaling concepts for the dynamics of viscous liquids near an ideal glassy state. *Phys Rev A* 40(2):1045–1054.
12. Götze W (2009) *Complex Dynamics of Glass-Forming Liquids* (Oxford Univ Press, Oxford).
13. Kurchan J, Parisi G, Urbani P, Zamponi F (2013) Exact theory of dense amorphous hard spheres in high dimension. II. The high density regime and the Gardner transition. *J Phys Chem B* 117(42):12979–12994.
14. Ikeda A, Miyazaki K (2010) Mode-coupling theory as a mean-field description of the glass transition. *Phys Rev Lett* 104(25):255704.
15. Cammarota C, Biroli G (2012) Ideal glass transitions by random pinning. *Proc Natl Acad Sci USA* 109(23):8850–8855.
16. Cammarota C, Biroli G (2013) Random pinning glass transition: Hallmarks, mean-field theory and renormalization group analysis. *J Chem Phys* 138:12A547.
17. Cammarota C (2013) A general approach to systems with randomly pinned particles: Unfolding and clarifying the random pinning glass transition. *EPL* 101(5):56001.
18. Berthier L, Kob W (2012) Static point-to-set correlations in glass-forming liquids. *Phys Rev E Stat Nonlin Soft Matter Phys* 85(1):011102.
19. Scheidler P, Kob W, Binder K (2004) The relaxation dynamics of a supercooled liquid confined by rough walls. *J Phys Chem B* 108(21):6673–6686.
20. Franz S, Parisi G (2013) Universality classes of critical points in constrained glasses. *J Stat Mech* 2013(11):P11012.
21. Kob W, Berthier L (2013) Probing a liquid to glass transition in equilibrium. *Phys Rev Lett* 110(24):245702.
22. Adam G, Gibbs JH (1965) On the temperature dependence of cooperative relaxation properties in glass-forming liquids. *J Chem Phys* 43(1):139–146.
23. Franz S, Parisi G (1997) Phase diagram of coupled glassy systems: A mean-field study. *Phys Rev Lett* 79(13):2486–2489.
24. Kob W, Andersen HC (1995) Testing mode-coupling theory for a supercooled binary Lennard-Jones mixture I: The van Hove correlation function. *Phys Rev E Stat Phys Plasmas Fluids Relat Interdiscip Topics* 51(5):4626–4641.
25. Stillinger FH, Weber TA (1982) Hidden structure in liquids. *Phys Rev A* 25(2):978–989.
26. Sciortino F, Kob W, Tartaglia P (1999) Inherent structure entropy of supercooled liquids. *Phys Rev Lett* 83(16):3214–3217.
27. Sciortino F (2005) Potential energy landscape description of supercooled liquids and glasses. *J Stat Mech* 2005(05):P05015.
28. Berthier L, Coslovich D (2014) Novel approach to numerical measurements of the configurational entropy in supercooled liquids. *Proc Natl Acad Sci USA* 111(32):11668–11672.
29. Sastry S, Debenedetti PG, Stillinger FH (1998) Signatures of distinct dynamical regimes in the energy landscape of a glass-forming liquid. *Nature* 393(6685):554–557.
30. Brumer Y, Reichman DR (2004) Mean-field theory, mode-coupling theory, and the onset temperature in supercooled liquids. *Phys Rev E Stat Nonlin Soft Matter Phys* 69(4):041202.
31. Kim K, Miyazaki K, Saito S (2011) Slow dynamics, dynamic heterogeneities, and fragility of supercooled liquids confined in random media. *J Phys Condens Matter* 23(23): 234123.
32. Ruocco G, Sciortino F, Zamponi F, De Michele C, Scopigno T (2004) Landscapes and fragilities. *J Chem Phys* 120(22):10666–10680.
33. Angelani L, Ruocco G, Scala A, Sciortino F, Di Leonardo R (2000) Saddles in the energy landscape probed by supercooled liquids. *Phys Rev Lett* 85(25):5356–5359.
34. Broderix K, Bhattacharya KK, Cavagna A, Zippelius A, Giardina I (2000) Energy landscape of a Lennard-Jones liquid: Statistics of stationary points. *Phys Rev Lett* 85(25):5360–5363.
35. Widom B (1965) Equation of state in the neighborhood of the critical point. *J Chem Phys* 43(11):3898–3905.
36. Xu L, et al. (2005) Relation between the Widom line and the dynamic crossover in systems with a liquid-liquid phase transition. *Proc Natl Acad Sci USA* 102(46):16558–16562.
37. Garrahan JP (2014) Transition in coupled replicas may not imply a finite-temperature ideal glass transition in glass-forming systems. *Phys Rev E Stat Nonlin Soft Matter Phys* 89(3):030301.
38. Chakrabarty S, Karmakar S, Dasgupta C (2014) Phase diagram of glass forming liquids with randomly pinned particles. arXiv:1404.2701.
39. Nandi SK, Biroli G, Bouchaud J-P, Miyazaki K, Reichman DR (2014) Critical dynamical heterogeneities close to continuous second-order glass transitions. *Phys Rev Lett* 113(24):245701.
40. Biroli G, Cammarota C, Tarjus G, Tarzia M (2014) Random-field-like criticality in glass-forming liquids. *Phys Rev Lett* 112(17):175701.
41. Hukushima K, Nemoto K (1996) Exchange Monte Carlo method and application to spin glass simulations. *J Phys Soc Jpn* 65(6):1604–1608.
42. Berthier L, Kob W (2007) The Monte Carlo dynamics of a binary Lennard-Jones glass-forming mixture. *J Phys Condens Matter* 19(20):205130.
43. Coluzzi B, Parisi G, Verrocchio P (2000) Lennard-Jones binary mixture: A thermodynamical approach to glass transition. *J Chem Phys* 112(6):2933–2944.
44. Nocedal J, Wright SJ (1999) *Numerical Optimization* (Springer, Berlin).